Tellus (2006), 58A, 593–600
Printed in Singapore. All rights reserved

© 2006 The Authors
Journal compilation © 2006 Blackwell Munksgaard

TELLUS

Correlation properties of daily temperature anomalies over land

By ANDREA KIRÁLY, IMRE BARTOS and IMRE M. JÁNOSI*, *Department of Physics of Complex Systems, Loránd Eötvös University, Pázmány P. s. 1/A, H-1117 Budapest, Hungary*

(Manuscript received 8 February 2006; in final form 15 May 2006)

ABSTRACT

Several thousands of temperature records from the Global Daily Climatology Network are analysed by means of detrended fluctuation analysis (DFA). Long-range temporal power-law correlations extending up to several years are detected for each station. Contrary to earlier claims, the correlation exponent is not universal for continental locations. Short-range correlations are also evaluated by DFA and by first order autoregressive models. The strength of short- and long-range temporal correlations seems to be coupled for large geographic areas. The spatial patterns are quite complex, simple parameter dependence such as elevation or distance from oceans cannot explain the observed variability.

1. Introduction

It is well established that the limit for predictability of daily meteorological parameters does not exceed about two weeks. This short-term 'memory' of many atmospheric parameters are well approximated by low order autoregressive (AR) processes (von Storch et al., 1999). The success of AR models in summarizing observations and in simulations of large sets of stochastically similar data has concealed the fact that several atmospheric parameters exhibit long-range asymptotic correlations (Pelletier, 1997; Koscielny-Bunde et al., 1998; Tsonis et al., 1999; Talkner and Weber, 2000; Syroka and Toumi, 2001; Weber and Talkner, 2001; Caballero et al., 2002; Govindan et al., 2002; Király and Jánosi, 2002; Blender and Fraedrich, 2003; Eichner et al., 2003; Fraedrich and Blender, 2003; Monetti et al., 2003; Fraedrich et al., 2004a; Pattantyús-Ábrahám et al., 2004; Király and Jánosi, 2005; Müller and Jánosi, 2005). This finding has been strongly fostered by the development of new analytical tools such as the detrended fluctuation analysis (DFA) (Peng et al., 1994, 1995). The main benefit of DFA over traditional algorithms (autocorrelation function, Fourier analysis, Hurst analysis, etc.) is that non-stationary signals can be adequately evaluated, where the classical methods often give spurious results.

The discussion of long-range correlations in recent literature has been centered around a few key points. Firstly, Koscielny-Bunde et al. (1998) proposed that the asymptotic power-law correlations for temperature time-series might be universal having the same exponent irrespectively of the geographic location. Later, Weber and Talkner (2001), Eichner et al. (2003), Fraedrich and Blender (2003), Kurnaz (2004a,b) and Király and Jánosi (2005) have found a rather wide range of exponent values over land, not to mention the marked difference between land and sea surface temperatures (Fraedrich and Blender, 2003; Monetti et al., 2003; Fraedrich et al., 2004a). Further, Pattantyús-Ábrahám et al. (2004) reported different correlation exponents for daily minimum and maximum temperature records at several stations. In spite of the fact that an increasing number of evaluations seems to contradict the hypothesis of universality, the discussion has not yet shut down (Blender and Fraedrich, 2004; Bunde et al., 2004; Fraedrich and Blender, 2004b; Vyushin et al., 2004a).

The second point is a clear corollary of disapproving universality. If the correlation exponent depends on the location, then what is its geographic distribution? Király and Jánosi (2005) observed a simple pattern over the Australian continent, namely, the strength of asymptotic correlations decreases with the distance from the equator. Similar pattern was not identified by Fraedrich and Blender (2003), however their study has a rather low spatial resolution. A search for systematic dependence on the distance from the oceans (Eichner et al., 2003; Király and Jánosi, 2005) or on elevation (Király and Jánosi, 2005) gave negative results.

The third important point concerns simulations by global coupled climate models. Govindan et al. (2002) reported that leading numeric models failed to reproduce long-range temporal correlations for temperature data. Fraedrich and Blender showed that an improved representation of atmosphere-ocean coupling results in better model performance, both with constant atmospheric greenhouse gas concentration (Fraedrich and Blender, 2003) or

*Corresponding author.
e-mail: janosi@lecso.elte.hu
DOI: 10.1111/j.1600-0870.2006.00195.x

with the IPCC scenario IS92a (Blender and Fraedrich, 2003). Vyushin et al. (2004a) found that inclusion of volcanic forcing helps to reproduce scaling behaviour in the NCAR-PCM model. Reproductive power of global models is an important question especially at interpreting climate change predictions.

In this work, we provide a comprehensive analysis of correlation properties for surface temperature data in the Global Daily Climatology Network (GDCN). We consider both short- and long-term correlations by means of detrended fluctuation analysis. We show that temperature records obey significant asymptotic power-law correlations at each geographic location over land. The scaling is not universal, lower and higher correlation exponent values are spatially clustered. We found that short- and long-range correlations are coupled for many geographic areas. An extended analysis of dependence on elevation and distance from oceans gave negative results, the observed geographic patterns require a more complex climatological explanation.

2. Data and methods

We have evaluated surface temperature records from the GDCN data set collected by the NOAA National Climatic Data Center's Climate Analysis Branch (http://www.ncdc.noaa.gov/oa/climate/research/gdcn/gdcn.html). We concentrated our analysis on the 9431 stations (out of the total 14 767) where the number of recorded daily minimum and maximum temperatures exceeds 8000 (approximately 22 yr). Various filtering methods decreased the number of stations further, details are presented at the specific results.

The DFA method has been exhaustively described in dozens of papers, therefore here we settle for a short summary of it.

As a first step of the analysis, the annual cycle is removed from the daily temperature values by the long-time climatological average for the given calendar day, as usual. Note that this procedure, which provides the temperature anomaly data a_i, cannot remove slow trends from the original time-series, such as a gradual shift of the annual means. Next we consider the anomaly series as increments of a random walk process. The 'trajectory' or 'profile' of the signal is given by simple summation as $y_j = \sum_{i=1}^{j} a_i$. We divide the profile into non-overlapping segments of equal length n. In each segment, the local trend is fitted by a polynomial of order p and the profile is detrended by subtracting this local fit. The usual measure of fluctuations is the standard deviation of the detrended segment averaged over all the segments $\langle F_p(n)\rangle$. A power-law relationship between $\langle F_p(n)\rangle$ and n indicates scaling with an exponent δ (DFAp exponent):

$$\langle F_p(n)\rangle \sim n^{\delta}. \tag{1}$$

Note that such a process has power-law autocorrelation function and power spectrum

$$C(\tau) = \langle a_i a_{i+\tau}\rangle \sim \tau^{-\alpha}, \qquad S(f) \sim f^{-\beta}, \tag{2}$$

where $0 < \alpha < 1$ and $0 < \beta < 1$. The relationships between the correlation exponents are (Koscielny-Bunde et al., 1998; Talkner and Weber, 2000)

$$\alpha = 2(1-\delta), \qquad \beta = 2\delta - 1. \tag{3}$$

Consequently, long-memory (persistent) processes are characterized by a DFA exponent $\delta > 1/2$, uncorrelated time-series (e.g. pure random walk) obey $\delta = 1/2$, antipersistent signals have $\delta < 1/2$. (Here the terms 'persistent' and 'antipersistent' are used in the sense that an increasing trend in the past implies an increasing or decreasing trend in the future, thus it slightly differs from 'persistence' in climatology defined as the continuance of a specific pattern.)

Talkner and Weber (2000) and Heneghan and McDarby (2000) pointed out that DFA and traditional power spectra provide equivalent characterizations of correlated stochastic signals, with the essential difference that DFA can effectively filter out slow trends. Local polynomial fits of order p eliminate polynomial background trends of order $p-1$. In practice, asymptotic correlation is inferred when the exponent δ does not depend on p.

Systematic analyses by Hu et al. (2001), Kantelhardt et al. (2001), Chen et al. (2002, 2005) and Xu et al. (2005) with various synthetic time-series revealed many useful details on the efficiency of the method. One of the main findings is that DFA curves for signals with different correlation properties and background trends can be fully explained by the assumption of variance superposition. An important result concerns missing intervals (very common in data bases). If a record has positive long-range correlations ($\delta > 1/2$), segments up to 50% of the total length can be removed. DFA tests on the rest stitched together show the same scaling behaviour as the whole record (Chen et al., 2002).

Figure 1a shows a typical DFA curve for a given station. The results for each station share common features. There is a marked crossover from an initial large slope regime to a longer straight segment of steepness larger than $1/2$ in the double-logarithmic plots. The crossover time is $n \approx 12$–20 d in agreement with the expectations. Fig. 1b illustrates the corresponding power spectrum. The theoretical relationship eq. (3) seems to be approximated well for low frequencies, however the drop of resolution and possible non-stationarities in the record make a quantitative estimate much more inaccurate than with DFA.

We evaluated also initial slopes reflecting short-range correlation properties, therefore we implemented a correction procedure proposed by Kantelhardt et al. (2001). This is necessary because local trend removal in small n windows introduces a bias towards too small residual fluctuations. Exploiting the fact that the correction function has a weak dependence on asymptotic properties (Kantelhardt et al., 2001), we used an effective correction by simulating long uncorrelated sequences. Such an artificial signal should have a DFA slope of $1/2$ everywhere. We tabulated the differences between the expected and measured curves, and we employed these values to correct raw DFA results.

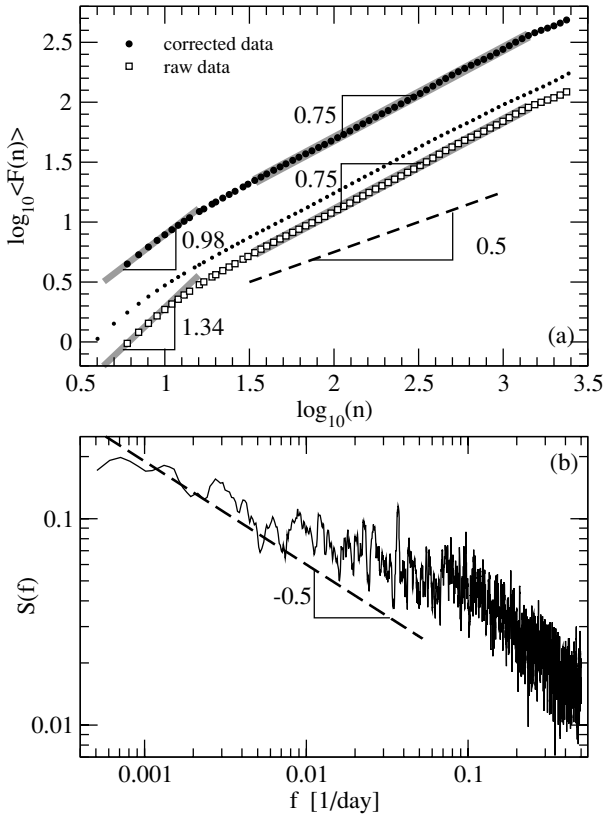

Fig. 1. (a) Typical DFA2 curve for daily temperature anomaly data (Gunnedah 1969–1995, 31.02°S, 150.27°E): logarithm of the average fluctuations $\log_{10}\langle F(n)\rangle$ versus logarithm of window size $\log_{10}(n)$. (Dotted line shows the DFA1 curve for comparison.) The raw data (empty squares) are corrected for short times (black circles, shifted upward) as proposed by Kantelhardt et al. (2001), see text. Initial and asymptotic slopes are indicated, as well as the slope 1/2 for an uncorrelated stochastic process (dashed line). (b) Power spectrum for the same anomaly series on double logarithmic scales. Dashed line indicates the theoretical expectation from eq. (3), it is *not* fitted.

Depending on the total length of the record N, the sampling statistics breaks down at window sizes $n \sim 0.25N$. We systematically checked local linear (DFA1), quadratic (DFA2) and cubic (DFA3) detrending in order to compare asymptotic exponents. We observed small changes between DFA1 and DFA2 values for a few cases, but no difference between DFA2 and DFA3 exponents.

The initial steep part of DFA curves indicates strong correlations for short-time intervals. This behaviour is successfully described by simple AR1 models as

$$a_{i+1} = Aa_i + \sigma\zeta_i, \tag{4}$$

where $A < 1$ for stationarity, and σ^2 is the variance of the uncorrelated, zero mean Gaussian noise term ζ. The coefficients A and σ can be estimated for empirical data by means of standard methods included in every statistical software. The autocorrelation function decays exponentially:

$$C_1(\tau) = \langle a_i a_{i+\tau}\rangle = \frac{\sigma^2}{1-A^2}A^\tau. \tag{5}$$

Such an exponential correlation function is reflected by a DFA curve of gradually decreasing slope, however the initial few points can be evaluated by a linear fit in a double-logarithmic plot (see Fig. 1a). The asymptotic exponent for pure AR1 signals always converges to $\delta = 1/2$. A transparent measure of short-range 'memory' is the decorrelation time or integral timescale $T_{\rm d}$ (von Storch et al., 1999)

$$T_{\rm d} = 1 + 2\sum_{\tau=1}^{\infty}\frac{C_1(\tau)}{C_1(0)} = \frac{1+A}{1-A}. \tag{6}$$

A similar correlation sum for a power-law eq. (2) is obviously divergent.

3. Results

Since thousands of DFA curves cannot be inspected individually, we paid special attention to control the fitting procedure. We tested the algorithms for two sets: time-series of at least 8000 recorded data with maximum 40% of missing intervals (8260 stations), and a subset of it containing missing intervals shorter than 5 d (3315 stations). Missing data were complemented by linear interpolation for the later subset, the rest was evaluated by the method of cutting and stitching (see in the previous section). Linear fits for the DFA curves were performed in the range $n = 18, \ldots, 1800$ d for windows of 21 logarithmically spaced points. This window slid over the range resulting in 33 individual slopes, which allowed to estimate fitting errors. The histogram of errors on exponent values (not shown here) has a highly peaked shape centered around 0.05, which agrees completely with the error estimates by Fraedrich and Blender (2003).

The statistics for asymptotic DFA2 exponents is shown in Fig. 2. The normalized frequency distributions are very similar both for daily maximum and minimum temperatures. Note that values lower than 0.6 were detected for 0.78% of the stations only, which seems to be negligible. This indicates the existence of long-range positive correlations everywhere over land. The distribution of differences ($\delta^{\max} - \delta^{\min}$) is plotted in Fig. 2c. Significant differences, where the error bars do not overlap for the two exponent values are found for ~2% of the stations. We could not identify any systematic dependence on geographic parameters or spatial correlation for stations of large exponent-deviation, similarly to earlier studies on a much smaller sample (Pattantyús-Ábrahám et al., 2004).

The universality hypothesis (Koscielny-Bunde et al., 1998) cannot be challenged by means of the histograms alone (Figs. 2a and b). However, Fig. 3 shows that lower and higher values have strong geographic correlations. The pattern is not

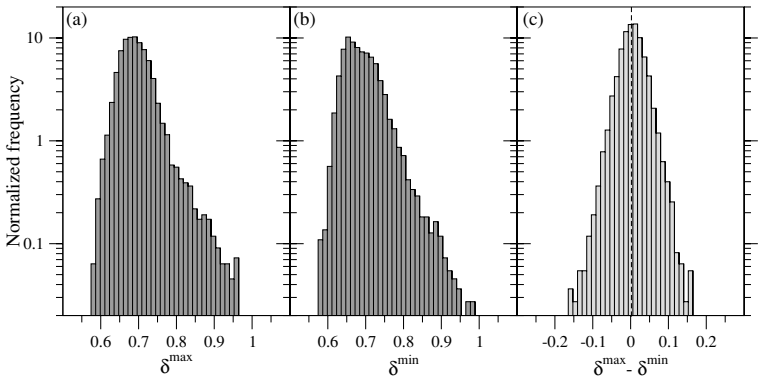

Fig. 2. Normalized histogram of (a) asymptotic DFA2 exponents for daily maxima $\delta^{\max}$, (b) the same for daily minima $\delta^{\min}$, and (c) the same for the differences $\delta^{\max} - \delta^{\min}$ for each station.

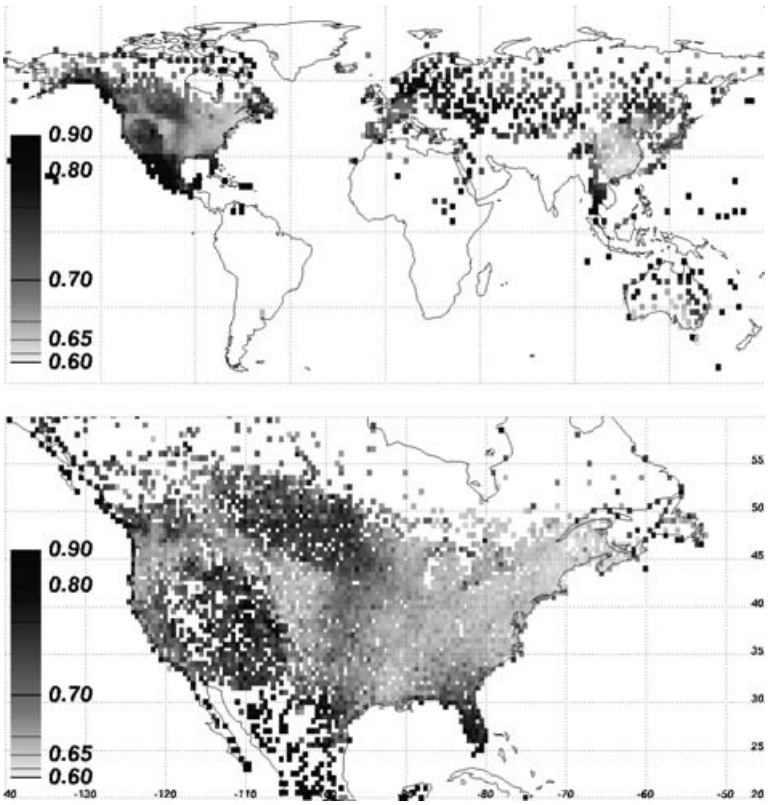

Fig. 3. Distribution of DFA2 asymptotic exponents $\delta^{\max}$ for stations of more than 8000 recorded daily maximum temperatures. The grayness scale is approximately logarithmic. Top: global data averaged over 2×2 degrees. Bottom: North American data averaged over 0.5×0.5 degrees.

so simple as over Australia (Király and Jánosi, 2005). Unfortunately data is practically not available for Africa and South America, but it seems that the western boundaries of ocean basins exhibit lower values (weaker apparent long-range correlations).

The geographic distribution of asymptotic correlation exponents for daily minimum temperatures $\delta^{\min}$ is essentially the same as for $\delta^{\max}$ (Fig. 3).

Next we evaluated the initial slopes of DFA2 curves (see Fig. 1a) for the same set of stations, the statistics is shown in Fig. 4. Here the similarity of the histogram shapes for daily maxima and minima is weaker than that of the asymptotic exponents in Fig. 2. Furthermore, the deviation $\delta_0^{\max} - \delta_0^{\min}$ has an asymmetric distribution shifted toward positive values. Alike to the asymptotic case, we could not identify a clear spatial pattern for the differences of initial exponents. The apparent differences in correlation properties for daily maxima and minima might depend on local microclimatic circumstances, however an adequate explanation requires further work.

The initial exponents $\delta_0^{\max}$ and $\delta_0^{\min}$ themselves exhibit correlated geographic patterns, we show the results for daily maxima in Fig. 5. (Again, the maps are practically the same for $\delta_0^{\min}$.)

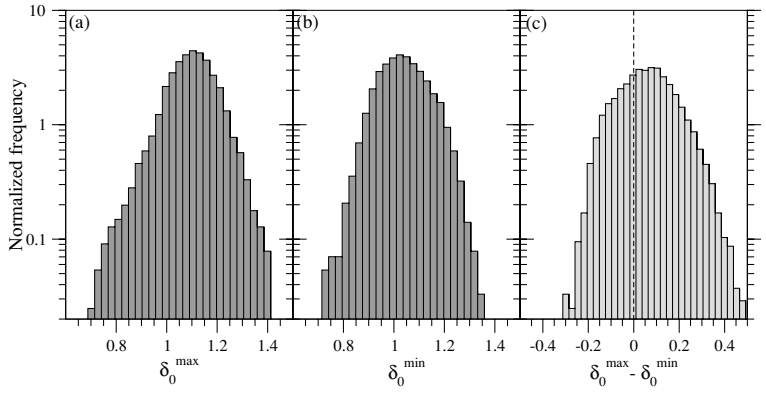

Fig. 4. Normalized histogram of (a) corrected initial DFA2 exponents for daily maxima $\delta_0^{\max}$, (b) the same for daily minima $\delta_0^{\min}$, and (c) the same for the differences $\delta_0^{\max} - \delta_0^{\min}$ for each station.

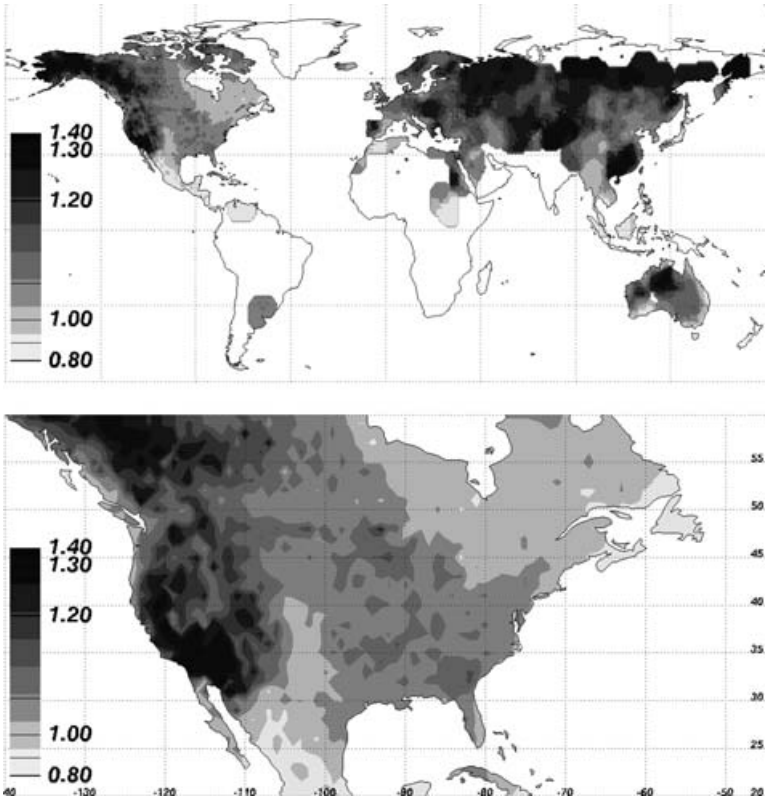

Fig. 5. Distribution of corrected DFA2 initial exponents $\delta_0^{\max}$ for stations of more than 8000 recorded daily maximum temperatures. The grayness scale is approximately logarithmic. The spatial resolution is the same as in Fig. 3, interpolated mapping. Top: global data. Bottom: zoomed to North America.

A direct comparison of Figs. 3 and 5 does not reveal too strong coupling between the different timescales, apart from the existence of large spatially correlated regions. But a possible connection between short- and long-range correlations is an important question, therefore we return to this point in the next section.

Since short-range correlations are usually modeled by autoregressive processes, we evaluated the same records by fitting AR1 coefficients as well. It is obvious that an AR1 process cannot reproduce all the statistical features of temperature records, especially long-range correlations (Király and Jánosi, 2002), but it gives a satisfactory first approximation when only short-range correlations are considered (von Storch et al., 1999; Bartos and Jánosi, 2005). The geographic distribution of AR1 coefficients is shown in Fig. 6. The similarity of these patterns to Fig. 5 is evident.

4. Discussion

The mathematical definition of long-range correlations comprises that the correlation sum is divergent. However, any finite sequence has finite correlation sum, furthermore any evaluation of a finite time-series cannot disregard the appearance of two natural timescales: the shortest scale is the sampling period, and the longest scale is the total length of the observations. Even more, when atmospheric correlations are discussed, another timescale is implicitly present, namely the human time-scale. When

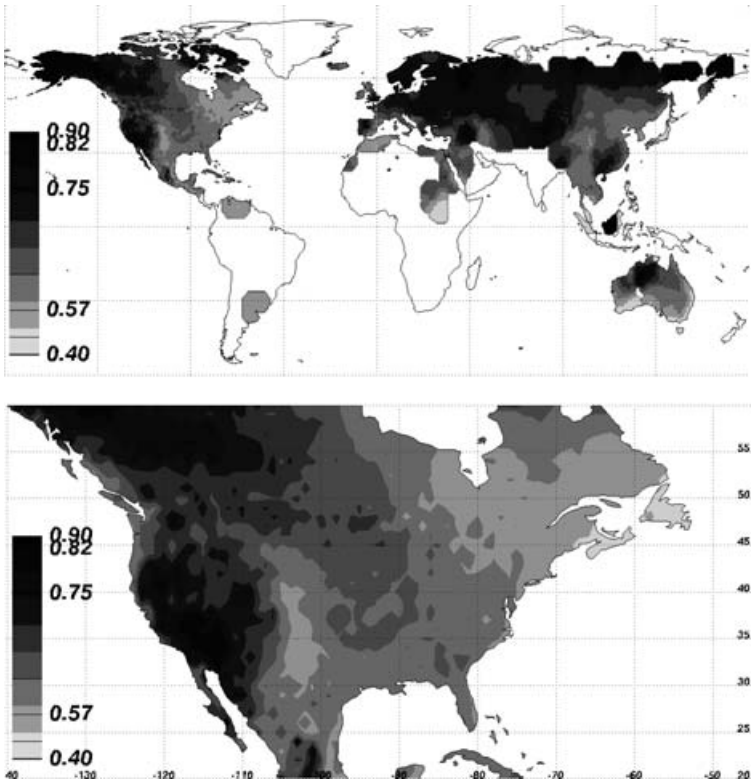

Fig. 6. Distribution of fitted autoregressive coefficient A (see eq. 4) for stations of more than 8000 recorded daily maximum temperatures. The grayness scale is approximately logarithmic. Top: global data. Bottom: zoomed to North America.

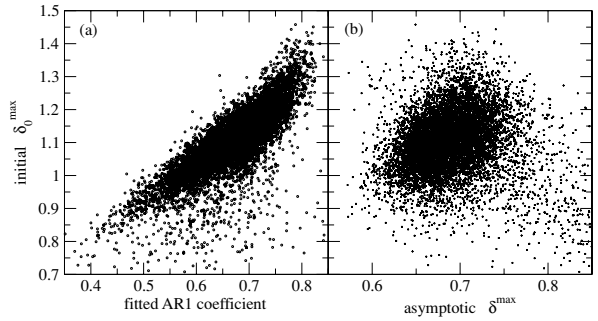

Fig. 7. Correlation plot for the initial DFA2 exponent $\delta_0^{\max}$ with (a) the fitted autoregressive coefficient A (see eq. 4), and with (b) the asymptotic exponent $\delta^{\max}$.

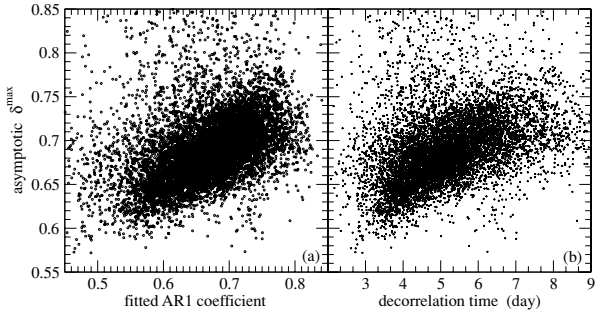

Fig. 8. Asymptotic DFA2 exponent $\delta^{\max}$ for daily maximum temperature anomalies versus (a) fitted AR1 coefficient A, and (b) decorrelation time T_{d}.

fluctuations are found to be correlated in an interval of several years, this can be regarded as 'long-range' compared to the 'short-range' memory of weather phenomena. Nevertheless, the long-range memory cannot be infinite, thus DFA exponents of long enough records should ultimately converge to $1/2$. This might explain why Fraedrich and Blender (2003) observed smaller exponent values in monthly data extending over 150 yr.

The similar geographic distributions of initial DFA2 slopes $\delta_0^{\max}$ (Fig. 5) and AR1 coefficients A (Fig. 6) indicate that both methods detect the strong short-range autocorrelation in daily temperature anomaly records. Indeed, Fig. 7a shows that the two characteristics are interrelated. We note however that the relationship is not obvious: computer generated AR1 data evaluated by DFA method did not reproduce the approximately linear correlation between A and δ_0 visible in Fig. 7a. Apart from the inherent noise in the records, the markedly different asymptotic properties of pure AR1 and real data may also contribute to the deviations.

The correlation plot for the initial and asymptotic slopes, δ_0 and δ (see Fig. 7b for daily maximum values) indicates the lack of a manifest connection. This is already suggested by the dissimilarity of maps Figs. 3 and 5. Therefore, it is remarkable that the correlation plots for asymptotic DFA2 exponents $\delta^{\max}$ with A or its transformed version T_{d} (see eq. 6) shown in Fig. 8 exhibit more structure. This result is further supported by checking the geographic patterns. As an example, we show the map for

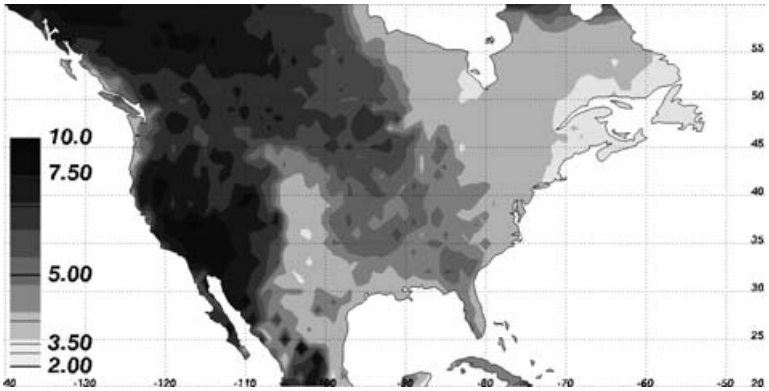

Fig. 9. Distribution of the decorrelation time T_d over North America, see eq. (6). (Interpolated mapping.)

the decorrelation time T_d over North America (where the spatial coverage is outstanding) in Fig. 9, which is to be compared with Fig. 3. The gross features are similar, however there are large areas where coherent discrepancies can be identified, e.g. over Florida, Mexico, the North Western coastline of the continent, or South East China and Japan (not shown here).

The patterns in the maps cannot be explained easily, especially because the spatial coverage of GDCN data is very uneven. It is clear that simple parameterizations, such as dependence on latitude, longitude, or the distance from oceans cannot describe the ramified distribution of exponent values. A clear dependence on elevation should be visible as topographic contours in the maps. A detailed statistics (not shown here) is in agreement with the suspicion that elevation is not a determinative parameter of apparent correlation properties.

The results in Figs. 8 and 9 suggest that there is a global relationship between short- and long-range correlations modified by local conditions. Further work is needed to reveal the nature of such connection, where globally coupled numeric models can help a lot.

5. Acknowledgments

This work was supported by the Hungarian Science Foundation (OTKA) under Grant Nos. T047233 and TS044839. IMJ thanks for a János Bolyai Research Scholarship of the Hungarian Academy of Sciences.

References

Bartos, I. and Jánosi, I. M. 2005. Atmospheric response function over land: Strong asymmetries in daily temperature fluctuations. *Geophys. Res. Lett.* **32**, L23820.

Blender, R. and Fraedrich, K. 2003. Long time memory in global warming simulations. *Geophys. Res. Lett.* **30**, L1769.

Blender, R. and Fraedrich, K. 2004. Comment on 'Volcanic forcing improves atmosphere-ocean coupled general circulation model scaling performance' by D. Vyushin, I. Zhidkov, S. Havlin, A. Bunde, and S. Brenner. *Geophys. Res. Lett.* **31**, L22213.

Bunde, A., Eichner, J. F., Havlin, S., Koscielny-Bunde, E., Schellnhuber, H. J. and co-author. 2004. Comment on Scaling of atmosphere and ocean temperature correlations in observations and climate models. *Phys. Rev. Lett.* **92**, 039801.

Caballero, R., Jewson, S. and Brix, A. 2002. Long memory in surface air temperature: detection, modeling, and application to weather derivative valuation. *Clim. Res.* **21**, 127–140.

Chen, Z., Ivanov, P. C., Hu, K. and Stanley, H. E. 2002. Effect of nonstationarities on detrended fluctuation analysis. *Phys. Rev. E* **65**, 041107.

Chen, Z., Hu, K., Carpena, P., Bernaola-Galvan, P., Stanley, H. E. and co-authors. 2005. Effect of nonlinear filters on detrended fluctuation analysis. *Phys. Rev. E* **71**, 011104.

Eichner, J. F., Koscielny-Bunde, E., Bunde, A., Havlin, S. and Schellnhuber, H. J. 2003. Power-law persistence and trends in the atmosphere: A detailed study of long temperature records. *Phys. Rev. E* **68**, 046133.

Fraedrich, K. and Blender, R. 2003. Scaling of atmosphere and ocean temperature correlations in observations and climate models. *Phys. Rev. Lett.* **90**, 108501.

Fraedrich, K., Luksch, U. and Blender, R. 2004a. 1/f model for long-time memory of the ocean surface temperature. *Phys. Rev. E* **70**, 037301.

Fraedrich, K. and Blender, R. 2004b. Reply to the comment on scaling of atmosphere and ocean temperature correlations in observations and climate models. *Phys. Rev. Lett.* **92**, 039802.

Govindan, R.B., Vyushin, D., Bunde, A., Brenner, S., Havlin S., and co-authors. 2002. Global climate models violate scaling of the observed atmospheric variability. *Phys. Rev. Lett.* **89**, 028501.

Heneghan, C. and McDarby, G. 2000. Establishing the relation between detrended fluctuation analysis and power spectral density analysis for stochastic processes. *Phys. Rev. E* **62**, 6103–6110.

Hu, K., Ivanov, P. C., Chen, Z., Carpena, P. and Stanley, H. E. 2001. Effect of trends on detrended fluctuation analysis. *Phys. Rev. E* **64**, 011114.

Kantelhardt, J. W., Koscielny-Bunde, E., Rego, H. H. A., Havlin, S. and Bunde, A. 2001. Detecting long-range correlations with detrended fluctuation analysis. *Physica A*, **295**, 441–454.

Király, A. and Jánosi, I. M. 2002. Stochastic modeling of daily temperature fluctuations. *Phys. Rev. E* **65**, 051102.

Király, A. and Jánosi, I. M. 2005. Detrended fluctuation analysis of daily temperature records: Geographic dependence over Australia. *Meteorol. Atmos. Phys.* **88**, 119–128.

Koscielny-Bunde, E., Bunde, A., Havlin, S., Roman, H. E., Goldreich, Y. and co-authors. 1998. Indication of universal persistence law governing atmospheric variability. *Phys. Rev. Lett.* **81**, 729–732.

Kurnaz, M. L. 2004a. Application of detrended fluctuation analysis to monthly average of the maximum daily temperatures to resolve different climates. *Fractals* **12**, 365–373.

Kurnaz, M. L. 2004b. Detrended fluctuation analysis as a statistical tool to monitor the climate. *J. Stat. Mech.: Theor. Exp.* **2004**, P07009.

Monetti, R. A., Havlin, S. and Bunde, A. 2003. Long term persistence in the sea surface temperature fluctuations. *Physica A* **320**, 581–589.

Müller, R. and Jánosi, I. M. 2005. Empirical mode decomposition and correlation properties of long daily ozone records. *Phys. Rev. E* **71**, 056126.

Pattantyús-Ábrahám, M., Király, A. and Jánosi, I. M. 2004. Nonuniversal atmospheric persistence: different scaling of daily minimum and maximum temperatures. *Phys. Rev. E* **69**, 021110.

Pelletier, J. D. 1997. Analysis and modeling of the natural variability of climate. *J. Climate* **10**, 1331–1342.

Peng, C. K., Buldyrev, S. V., Havlin, S., Simons, M., Stanley, H. E. and co-authors. 1994. Mosaic organization of DNA nucleotides. *Phys. Rev. E* **49**, 1685–1689.

Peng, C. K., Havlin, S., Stanley, H. E. and Goldberger, A. L. 1995. Quantification of scaling exponents and crossover phenomena in nonstationary heartbeat time series. *Chaos* **5**, 82–87.

Syroka, J. and Toumi, R. 2001. Scaling and persistence in observed and modeled surface temperature. *Geophys. Res. Lett.* **28**, 3255–3258.

Talkner, P. and Weber, R. O. 2000. Power spectrum and detrended fluctuation analysis: application to daily temperatures. *Phys. Rev. E* **62**, 150–160.

Tsonis, A. A., Roebber, P. J. and Elsner, J. B. 1999. Long-range correlations in the extratropical atmospheric circulation: Origin and implications. *J. Climate* **12**, 1534–1541.

von Storch, H. and Zwiers, F. W. 1999. *Statistical Analysis in Climate Research*. Cambridge University Press, Cambridge.

Vyushin, D., Zhidkov, I., Havlin, S., Bunde, A. and Brenner, S. 2004a. Volcanic forcing improves atmosphere-ocean coupled general circulation model scaling performance. *Geophys. Res. Lett.* **31**, L10206.

Vyushin, D., Zhidkov, I., Havlin, S., Bunde, A. and Brenner, S. 2004b. Reply to comment by R. Blender and K. Fraedrich on 'Volcanic forcing improves atmosphere-ocean coupled general circulation model scaling performance'. *Geophys. Res. Lett.* **31**, L22210.

Weber, R. O. and Talkner, P. 2001. Spectra and correlations of climate data from days to decades. *J. Geophys. Res. D* **106**, 20 131–20 144.

Xu, L. M., Ivanov, P. C., Hu, K., Chen, Z., Carbone, A. and Stanley, H. E. 2005. Quantifying signals with power-law correlations: A comparative study of detrended fluctuation analysis and detrended moving average techniques. *Phys. Rev. E* **71**, 051101.